

SIGNAL RECONSTRUCTION IN A HIGH RATE ENVIRONMENT FOR SCINTILLATOR CALORIMETERS

*E. Fullana, J. Castelo, V. Castillo, C. Cuenca, A. Ferrer, E. Higon, C. Iglesias,
A. Munar, J. Poveda, A. Ruiz-Martinez, B. Salvachua, C. Solans, R. Teuscher, J. Valls*

Departamento de Física Atómica, Molecular y Nuclear and IFIC, CSIC-Universidad de Valencia

ABSTRACT

We present an algorithm to reconstruct online the energy in the TiCal detector of ATLAS. The algorithm consists in weighted sums of the digital samples of the photomultiplier signal. The weights are calculated to reconstruct the desired parameters of the signal while minimizing the noise impact on the resolution. The algorithm has been satisfactorily tested in two types of data, data obtained with a charge injection calibration system and real physics data. The results are promising given significant improvements specially when the signal to noise ratio is small as it has been designed for.

1. INTRODUCTION

The LHC is the new proton-proton collider which is being built at CERN (European Organization for Nuclear Research) and will be operative in 2007 [1]. The LHC is designed to reach energies of 14 TeV in the center of mass frame. The LHC will produce an average of ~ 23 collisions every 25 ns. These features challenge the detectors placed around the collider in order to exploit the new physics discovery potential.

ATLAS is one of the four main detectors placed around the LHC [2]. It basically consists of several layers of cylindrical shaped subdetectors placed concentrically at the collision point. Every subdetector is segmented into channels which produce an electronic signal when a particle crosses the channel region. One of the subdetectors is the calorimeter which measures the energy of the particles that reach this layer of the detector.

2. SIGNALS IN CALORIMETRY

Each channel of the calorimeter produces an electrical signal proportional to the energy deposited in the region defined by that channel. Essentially, there are two technologies to produce such a signal. The first technology is based on the ionization of a liquid. The particle to be measured produces a set of pairs ion-electron which are attracted to

anodes by an electrical field. This signal is collected, shaped and digitalized. The second technology is based on the property of some materials of producing scintillating light when a charged particle goes through them. The light produced is driven through optical fibers to photomultipliers. The photomultipliers produce an electrical signal from this light by the combination of the photoelectric effect and electronic cascade. As in the previous case the electrical signal is shaped and digitalized. Before the shaper, the signals in liquid ionization calorimeters long of the order of hundreds of nanoseconds whereas the scintillator calorimeters signals long of the order of tens of nanoseconds. The shaper shortens the signal of the liquid ionization calorimeters and prolongs the signal of the scintillator calorimeter in order to accommodate them to a common read out.

The signals contain information of an interesting event selected by the trigger of the detector and also contribution from the 23 soft events produced simultaneously in each collision. These soft events are not interesting for high energy physics studies and their contribution degrades the signal, therefore they are treated as coherent noise, so called pile up noise. The shapers of liquid ionization calorimetry set the integration time of the signal. The ratio electronic noise to signal is inversely proportional to the integration time for the other hand the ratio pile up noise to signal is proportional to this time. Therefore there is an optimal integration time which minimizes the contribution of both signals. This is not the case for scintillator calorimeters the signal of which is shorter than the LHC period however once the shaper extends it the contribution of pile up noise increases.

The ATLAS calorimeter uses both technologies, the liquid ionization one to measure the energy of electrons, photons and hadrons (called LiAr calorimeter) and the scintillator one to measure the energy of hadrons (Tile calorimeter or TileCal) [3]. In both systems the digitization period is defined by the LHC clock, 25 ns and the digital samples are driven out from the detectors through optical links. At the back-end of the detector custom designed electronic cards, the RODs, read out the digital samples and reconstruct the original information of the signal. This information is ba-

sically the amplitude of the signal since it is proportional to the energy of the particle. The main requirement at this point is the computing time set by the first trigger latency which is about $10 \mu\text{s}$ in the ATLAS detector.

3. THE OPTIMAL FILTERING ALGORITHM

The Optimal Filtering algorithm (OF) inputs the digital samples of the signal and outputs signal related parameters, as amplitude or time information, as a result of the weighted sums of the samples. It consists in basic operations (sums and products) which make it suitable at ROD level where the computing time is limited. OF algorithm was first developed to be used in liquid ionization calorimeters. The integration time is set hardwired in the shaper, however due to changes in the luminosity of the accelerator, ageing of electronic components or limited tolerance of capacitors and resistors the integration time may not be optimal. The OF algorithm minimizes the noise impact on the resolution at the level of optimized integration time [4].

The aim of this work is to test the performance of the algorithm for scintillator calorimeters, specifically the ATLAS Tile Calorimeter. In order to do that we introduce a new parameter, out of amplitude and time, to account for the fact that the signal in TileCal lays above a non zero baseline, this magnitude is called pedestal.

4. THEORETICAL BACKGROUND

Let's define \mathbf{g} as a set of values of the shape form function of the signal, $g(t)$, noise free and normalized to one in amplitude. The \mathbf{g} values are taken at times t_i , the time interval of which must be equal to the sampling period. The samples can thus be expressed as:

$$S_i = p + Ag(t_i + \tau) + n_i,$$

where S represents the digital samples, A is the true amplitude of the signal, τ accounts for a phase between the shape form factors and the samples, n_i is the noise contribution and p is the pedestal.

We can develop it in Taylor's series as:

$$S_i \simeq p + Ag(t_i) - A\tau g'(t_i) + n_i = p + Ag_i - A\tau g'_i + n_i,$$

Let's define now three quantities:

$$u = \sum_{i=1}^n a_i S_i, \quad v = \sum_{i=1}^n b_i S_i, \quad w = \sum_{i=1}^n c_i S_i,$$

where n is the number of samples and \mathbf{a} , \mathbf{b} and \mathbf{c} are free parameters of the algorithm called OF weights.

We set now two conditions:

- The expected values of u , v and w ($\langle u \rangle$, $\langle v \rangle$ and $\langle w \rangle$) for m events of equal amplitude, time and pedestal must be equal to A , $A\tau$ and p respectively.
- The distributions of u , v and w values are broaded by the noise. We require the parameters \mathbf{a} , \mathbf{b} and \mathbf{c} to be calculated so that they minimize the u , v and w variances.

The theoretical development of the algorithm supposes a stationary noise, i.e. the statistical averages of the noise terms must be time independent, otherwise the algorithm is not valid.

With these conditions and using the Lagrange multipliers method - to minimize a function imposing constraints - we obtain three sets of $n+3$ equations and $n+3$ unknowns. The three systems of equations are linear (due to the Taylor's expansion) and their solution are the parameters \mathbf{a} , \mathbf{b} and \mathbf{c} [5]:

$$\begin{pmatrix} R_{11} & R_{12} & \dots & R_{1n} & g_1 & g'_1 & 1 \\ R_{21} & R_{22} & \dots & R_{2n} & g_2 & g'_2 & 1 \\ \vdots & \vdots & \ddots & \vdots & \vdots & \vdots & \vdots \\ R_{n1} & R_{n2} & \dots & R_{nn} & g_n & g'_n & 1 \\ g_1 & g_2 & \dots & g_n & 0 & 0 & 0 \\ g'_1 & g'_2 & \dots & g'_n & 0 & 0 & 0 \\ 1 & 1 & \dots & 1 & 0 & 0 & 0 \end{pmatrix} \begin{pmatrix} a_1 \\ a_2 \\ \vdots \\ a_n \\ \lambda \\ \kappa \\ \epsilon \end{pmatrix} = \begin{pmatrix} 0 \\ 0 \\ \vdots \\ 0 \\ 1 \\ 0 \\ 0 \end{pmatrix},$$

where g_i and g'_i are the values of the shape form and its derivative respectively, a_i are the OF weights (the system for \mathbf{b} and \mathbf{c} weights is identical only the independent term changes), λ , κ , ϵ are the Lagrange multipliers and R_{ij} are terms of the noise autocorrelation matrix which can be calculated by:

$$R_{ij} = \frac{\sum (n_i - \langle n_i \rangle)(n_j - \langle n_j \rangle)}{\sqrt{\sum (n_i - \langle n_i \rangle)^2 \sum (n_j - \langle n_j \rangle)^2}},$$

where n_i are noise samples.

5. RESULTS

We have tested the algorithm using two types of data, charge injection data and physics data.

In the TileCal front-end electronics there is a calibration system which injects charge to the shaper emulating the photomultiplier. The injected charges range between zero and 800 pC and the injection start time also ranges to cover the 25 ns sampling period. These features make the charge injection system suitable to test our algorithm in both amplitude and time reconstruction.

Figure 1 shows the results of the algorithm for amplitude reconstruction. The results are compared with the Flat

Filtering algorithm (FF) which consists in a plain sum of the samples. The top plot shows the reconstructed charge versus the injected charge for the whole range of charges, both in picocoulombs. The points represent the average of the distribution of the reconstructed charge for each injected charge. The middle plot represents the residual of the points to the line which bisects the graph. Both plots show that both algorithms output on average a correct reconstructed charge. The bottom plot shows the resolution of the reconstruction versus the injected charge. The resolution is defined as the ratio between the standard deviation and the average of the distribution of the reconstructed charge. The plot shows the difference between the FF algorithm and the OF one. The resolution at high injected charges is similar for both algorithms, however as the injected charge decreases the OF algorithm plots better resolution. This is a consequence of the OF basic concepts, the algorithm is designed to minimize the noise impact on the resolution which is more important at low charges where the signal to noise ratio is small.

Figure 2 right shows the plots for the time reconstruction of the OF algorithm. The phase between the samples and the g values was fixed in 5 ns. The top plot shows the average of the reconstructed phase distribution and the bottom plot shows its standard deviation both versus the injected charge for the whole range of charges. Notice that the phase is well reconstructed for the whole range of charges having an accuracy of 200 ps.

For the physics data we use pions and electrons of several energies. The data was taken during testbeam periods using the SPS accelerator at H8 CERN facility. Now the total energy deposited in the calorimeter is computed. The energy distribution of the energy deposited in the calorimeter fits a Gaussian distribution. The resolution of the calorimeter is defined as the ratio between the sigma and the average of the distribution.

Figure 3 top shows the resolutions obtained with the OF and FF algorithm versus the momentum of the incident electron. As in the charge injection case the improvement of the OF algorithm happens at low energies where the ratio signal to noise is small and the noise degrades significantly the resolution. Figure 3 bottom shares the same result, now the resolution are in general worse than in the electron case due to the intrinsic fluctuations of the shower developed by the pion but again the OF algorithm improves the resolution at low energies.

6. CONCLUSIONS

The optimal filtering algorithm has been tested satisfactorily in two types of data. For the data obtained with charge injection runs the reconstruction is correct for both amplitude and time. At the same time the algorithm improves the res-

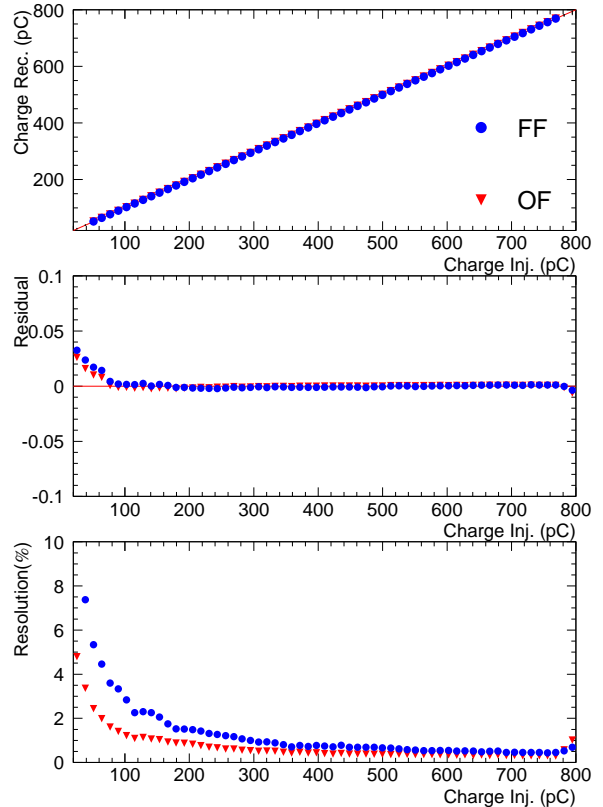


Fig. 1. Amplitude reconstruction for Optimal Filtering algorithm (OF) and Flat Filtering algorithm (FF).

olution, compared with plain filtering algorithms, when the signal to noise ratio is small. This result is shared in physics runs taken during physics calibration periods of the detector. Therefore the results are promising for the OF algorithm to be a good candidate to reconstruct online the energy of the Tile Calorimeter when the LHC will be operative.

7. ACKNOWLEDGMENTS

The authors would like to acknowledge the contribution of Bill Cleland for his wise advices and for sharing his wide knowledge about signal analysis. We also would like to express our gratitude to Rupert Leitner, Bob Stanek, Tomas Davidek and the people involved in the TileCal detector, specially the ones who contributed to the data acquisition and testbeam calibration period.

We would like also to thank Professor Hagit Messer-Yaron and David Primor for encouraging and giving us the chance to present this work in this workshop.

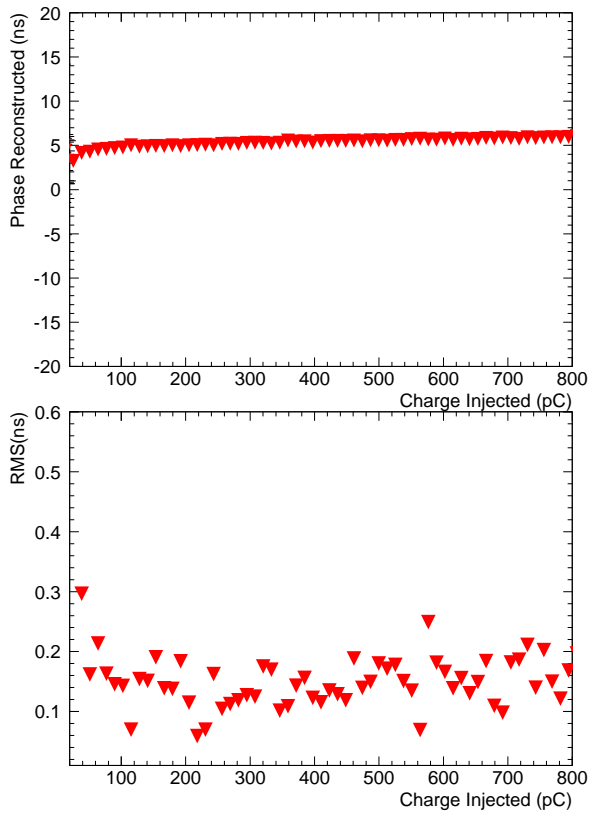


Fig. 2. Time reconstruction for Optimal Filtering algorithm (OF) and Flat Filtering algorithm (FF).

8. REFERENCES

- [1] J. Gareyte, "The LHC project," Prepared for International Europhysics Conference on High-energy Physics, Marseille, France, 22-28 Jul 1993.
- [2] ATLAS Collaboration, "ATLAS Technical Proposal," Tech. Rep. CERN/LHCC 94-43, CERN, 1994.
- [3] ATLAS Collaboration, "Calorimeter Performance Technical Design Report," Tech. Rep. CERN/LHCC 96-40, CERN, 1996.
- [4] W. E. Cleland and E. G. Stern, "Signal processing considerations for liquid ionization calorimeters in a high rate environment," *Nucl. Instr. Meth.*, vol. 338, pp. 467, 1994.
- [5] E. Fullana et al., "Optimal Filtering in the ATLAS Hadronic Tile Calorimeter," *ATLAS internal note, CERN-ATL-TILECAL-2005-001*, 2005.

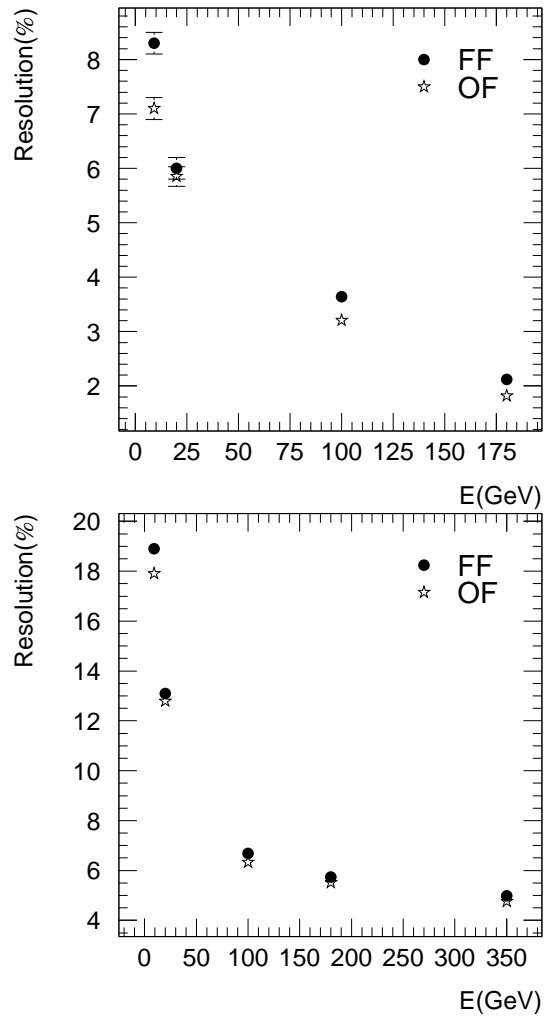


Fig. 3. Energy resolution of the TileCal detector obtained with the Optimal Filtering (OF) and Flat Filtering (FF) algorithm versus the momentum of the incident. The top plot shows the resolution for electrons whereas the bottom plot shows the resolution for pions.